CONF-940926--5

LOCAL TEXTURE AND GRAIN BOUNDARY MISORIENTATIONS IN HIGH J_C OXIDE SUPERCONDUCTORS

D. M. Kroeger[1], A. Goyal[1], and E. D. Specht[1], J. E. Tkaczyk[2], J. Sutliff[2], and J. A. DeLuca[2], Z. L. Wang[3], and G. N. Riley, Jr.[4]

[1]Metals and Ceramics Division, Oak Ridge National Laboratory, P. O. Box 2008, Oak Ridge, TN 37831 and [2]General Electric Corporate, Research and Development, P. O. Box 8, Schenectady, NY 12345

[3]National Institute of Standards and Technology, Metallurgy Division, Bldg. 223, Rm-B106, Gaithersburg, MD, and [4]American Superconductor Corporation, Westborough, MA 01581

ABSTRACT

The orientations of hundreds of contiguous grains in high J_C $TlBa_2Ca_2Cu_3O_x$ deposits and (Bi, Pb)$_2$ $Sr_2Ca_2Cu_3O_y$ powder-in-tube tapes have been determined from electron back scatter diffraction patterns (EBSP). The misorientation angles and axes of rotation (angle/axis pairs) for grain boundaries connecting these grains were calculated. For both materials the population of low angle boundaries was found to be much larger than expected from calculations based on their macroscopic texture. The $TlBa_2Ca_2Cu_3O_x$ deposits exhibit pronounced local texture which has been defined by EBSP and x-ray diffraction. Locally grains show significant in-plane (a-axis) alignment even though macroscopically a-axes are random, indicating the presence of colonies of grains with similar a-axis orientations. In (Bi, Pb)$_2$ $Sr_2Ca_2Cu_3O_x$ tapes no local texture was observed. In both materials the existence of connected networks of small angle grain boundaries can be inferred. Coincident site lattice (CSL) grain boundaries are also present in higher than expected numbers. Grain boundary energy thus appears to play a significant role in enhancing the population of potentially strongly-linked boundaries. We propose that long range strongly-linked conduction occurs through a percolative network small angle (and perhaps CSL) grain boundaries.

Proceedings of the Seventh New York State Institute Conference on Superconductivity and Applications, Buffalo, NY, September 7-9, 1994

1. INTRODUCTION

The microstructural determinants of critical current density, J_C, in polycrystalline oxide superconductors have been studied extensively in the course of development of processes for optimizing J_C. Long-range strongly-linked current flow in polycrystalline oxides is presently known to occur only in Bi-2223 [1] and Bi-2212 [2] conductors prepared by powder-in-tube and deposit approaches, in Tl-1223 deposits prepared by two-zone thallination [3, 4] and $YBa_2Cu_4O_8$ multifilament conductor prepared by the oxidation-of-metallic precursor process [5]. For all of these, the best J_C so far obtained is significantly smaller than the intrinsic or intragranular J_C, a fact which is generally attributed to weak link behavior at grain boundaries and/or to microcracks. The effects of grain boundary characteristics on current transmission across the boundary have been studied most extensively for $YBa_2Cu_3O_{7-x}$. For clean, stoichiometric grain boundaries, $J_{C(gb)}$, the grain boundary critical current, appears to be determined primarily by grain boundary misorientation. The dependence of J_C (gb) on misorientation angle has been determined in $YBa_2Cu_3O_{7-x}$ for grain boundary types which can be formed in epitaxial films on bicrystal substrates. These include [001] tilt, [100] tilt, and [100] twist boundaries [6, 7]. For this restricted set of boundaries the grain boundary plane does not appear to play an important role, although it should be noted that for none of the configurations tested was there a significant c-axis component to current flow. The low J_C invariably observed in randomly oriented polycrystalline material may be understood on the basis that grain boundaries with misorientations greater than about 10° are weakly linked and that the population of low angle grain boundaries is expected to be small. The finding that polycrystalline Bi-2212 and Bi-2223 conductors can be made which are strongly linked and carry high currents over macroscopic distances naturally raised the question of how they are different from Y123. Various ideas and models [8-15] for the path for strongly linked conduction have been discussed, including the possibility that grain boundaries in BSCCO are

fundamentally different from boundaries in Y123 [2, 15-17]. The most extensively discussed explanation for strongly linked current in BSCCO has been the brick-wall model [8, 9, 12, 13] in which large area [001] twist boundaries are seen as paths for current to flow around large angle weak-linked [001] tilt boundaries. However, measurements of the temperature dependence and anisotropy of J_C suggest that long-range current flow involves little or no c-axis conduction, and thus cast doubt upon the brick-wall mechanism [15, 18].

As an alternative to the brick-wall model Hensel et al. [15] have suggested that the numerous boundaries connecting grains which appear in polished cross-sections to have only modest c-axis misalignment are strongly linked in (Bi, Pb)$_2$ $Sr_2Ca_2Cu_3O_x$ PIT conductors. Current is envisioned to flow in "tracks" formed by a series of many such boundaries. In this "railway switch" model the assumptions of the brick-wall model are reversed. In the absence of c-axis conduction c-axis twist boundaries cannot be utilized, so boundaries with planes running approximately transverse to the current direction are assumed to be strongly-linked. The strong decrease of J_C with magnetic field is attributed not to weak links but to the anisotropy of J_C with respect to field direction and the presence of misaligned grains. They point out, as have Cho et al. [18], that in the absence of c-axis conduction misaligned grains provide a mechanism for making current flow three-dimensional. An apparent assumption of this model is that current transmission at grain boundaries in (Bi, Pb)-2223 is determined solely by c-axis misorientation, irrespective of relative basal plane orientation. This is in contrast to the known characteristics of Y123, for which, as discussed above, in-plane (i.e., a-axis) alignment within ~10° is required. Recently, Nabatami et al. [19] have performed J_C measurements on individual c-axis tilt grain boundaries in bicrystal $TlBa_2Ca_2Cu_3O_{8+x}$ deposits formed epitaxially on $SrTiO_3$ bicrystals and found that, as in Y123, grain boundaries with misorientation angles greater than about 10° are weak links. Furthermore, the limited data available on current transmission at grain boundaries in Bi-2212 indicate that most large angle [001] tilt and twist boundaries are weak links [6],

as in Y123. The increasing evidence that the characteristics of grain boundaries in Y123 are general makes desirable a model of strongly-linked current flow in polycrystalline material consistent with those characteristics.

Two important facts concerning high J_C polycrystalline Bi-based and Tl-based materials are that they have moderate to strong c-axis texture, and that their J_C's are only a small fraction of the intragranular J_C. As we will discuss below, an important consequence of c-axis texture is an increase in the population of small angle grain boundaries. These facts suggest the largely unexplored possibility that strongly-linked conduction occurs through a percolative network of small angle grain boundaries. To investigate this question we have calculated the distribution of grain boundary misorientation angles as a function of the degree of c-axis texture [20]. Also, we have measured using x-ray microdiffraction and electron back scatter diffraction patterns (EBSP), local textures and individual orientations of hundreds of contiguous grains in Bi-2223 powder-in-tube (PIT) conductor and Tl-1223 deposits. We find in the case of Bi-2223 PIT that the degree of c-axis texture present is not by itself sufficient to result in a high concentration of small angle boundaries. However, the actual population of small angle boundaries as determined from EBSP was higher than predicted, and apparently sufficient to provide a percolative path for strongly linked current. In the Tl-1223 deposits the population of small angle boundaries can be very high, ranging up to 80-90% of boundaries. It has been determined previously [21-23] that in these deposits grains are arranged in "colonies" within which grains have similar orientations. Within colonies nearly all grain boundaries have small misorientations and current flow is strongly linked. Long range conduction is thus limited by grain boundaries at colony intersections where the population of small angle boundaries may be much lower than inside a colony.

The high concentrations of low angle boundaries in both of these materials we attribute to the effects of grain boundary energy. In the Tl-1223 deposits we find that the population of coincident site lattice boundaries, which are expected to have low energy, as are small angle boundaries, is elevated. We propose that long-range current flow in polycrystalline oxide superconductors occurs by percolation through a network of low energy boundaries. Connectivity and therefore critical current density is determined not only by the population of low angle (and perhaps CSL) boundaries but also by their local arrangement, i.e., by the local texture.

2. COMPUTER SIMULATION OF THE MISORIENTATION DISTRIBUTION AS A FUNCTION OF MACROSCOPIC TEXTURE

Goyal et al. [20] have shown that the difficult geometrical problem of determining the distribution of misorientation angles for a polycrystalline material of any crystal symmetry can be solved by a conceptually simple numerical simulation. The method involves generating, from the Euler angle description of the orientation of a crystal, a set of randomly oriented grains, and then determining the angle-axis pairs which describe the misorientations between all of the pairs of grains which can be formed from the set. A set of 200 randomly oriented grains was used, resulting in nearly 20,000 grain boundaries. The misorientation between two grains can be described by an axis and the angle through which one of the grains must be rotated about this axis to align the grains. For a given crystal structure there is a set of equivalent angle-axis pairs which describe a given grain boundary misorientation. By convention; the pair with the smallest positive misorientation angle is chosen.

Figure 1 shows the distribution of misorientation angles obtained from the simulation of a randomly oriented polycrystalline cubic material. The shape of this histogram is in

good agreement with the theoretical calculation of Mackenzie [24]. The fraction of grain boundaries with misorientation angles less than a given angle can be obtained by summing and normalizing the results in Fig. 1, and is shown in Fig. 2 (solid curve). Similar curves are shown for tetragonal and orthorhombic materials. It is apparent that for all three the population of boundaries with misorientation angles less than 10° is small. Goyal et al. [20] have shown that specific macroscopic textures can be imposed on the set of grains from which grain boundaries are formed by restricting the range of values from which certain of the Euler angles describing grain orientations are randomly chosen. The effect of c-axis texture on the distribution of misorientation angles is shown in Fig. 3. The fraction of misorientation angles less than an angle Θ is plotted for cases in which the c-axes of grains are restricted to angular ranges of 10°, 20°, etc., and the a-axes are random and not restricted. The number of small angle boundaries increases as the range of variation of the c-axis orientation is decreased. For perfect c-axis alignment, 22.2% of boundaries would have misorientation angles less than 10°. Bi-2223 powder-in-tube conductors typically have c-axis rocking curves with full-width-at-half-maximum ~15-20°, suggesting that the 10° or 20° curves in Fig. 3 may apply to them, where as the Tl-1223 spray pyrolyzed deposits have FWHM ~1-2°. It should be stressed that these simulations yield misorientation angle distributions based solely upon geometry. Factors such as the variation of grain boundary energy with misorientation and grain boundary plane, grain morphology as determined by surface and interfacial energies, and processing factors may strongly affect the distribution of misorientation angles in a real material. As we will see below, this is indeed the case for the Tl-1223 deposits and Bi-2223 conductors we have examined.

3. EXPERIMENTAL DETERMINATION OF GRAIN BOUNDARY MISORIENTATION DISTRIBUTIONS

Since the distribution of grain boundary misorientations is not uniquely related to macroscopic texture (i.e. can be affected by grain boundary energies, etc.) it must be determined from measurements of the orientations of contiguous grains. The most rapid and efficient method for obtaining orientations of individual grains is electron back scatter diffraction. Using facilities at General Electric Corporate Research and Development Center and at TEXSEM Laboratories in Salt Lake City, Utah, the orientations of hundreds of contiguous grains were determined in Tl-1223 deposits and in Bi-2223 powder-in-tube conductor.

3.1. Bi(Pb)-2223 Powder-in-Tube Conductor

Multifilamentary Bi(Pb)-2223 conductors prepared by the oxide powder-in-tube method having $J_C \simeq 20{,}000$ A/cm^2 in self-field at 77 K were examined. Silver was removed from one side by chemical etching to expose filament surfaces. Figure 4 shows an SEM image of a filament surface. Most grain boundaries are clearly visible, permitting the determination of electron back scatter diffraction patterns from adjacent grains. Diffraction patterns were obtained for all of the grains which could be distinguished in several small areas containing from 15 to ~100 contiguous grains [25]. The dominant pole in the diffraction pattern exhibited 4-fold symmetry and was indexed as the [001] pole of the approximately tetragonal Bi-2223 subcell [26, 27]. From the absolute orientation of grains, grain boundary misorientations were calculated in the form of axis/angle pairs. Figure 5 shows the proportion of small angle and coincident site lattice boundaries found in an area containing 227 identifiable boundaries. More than 30% of the boundaries have misorientation angles less than 10°. The FWHM for the c-axis rocking curve from x-ray diffraction for this sample is ~20°, typical of Bi-2223

powder-in-tube conductors. From Fig. 3 we see that in a textured material in which the c-axis directions of grains are similarly restricted and grain orientations are not locally correlated fewer than 5% of grain boundaries would have misorientation angles less than 10°. The high concentration of small angle boundaries presumably results from the fact that small angle boundaries have lower energies. The properties and therefore the importance of coincidence site lattice (CSL) boundaries have not been determined, although there are indications that some CSL boundaries may be better than other large angle boundaries [28]. The data in Fig. 5 suggest that their numbers are only slightly enhanced in PIT Bi-2223. That ~30% of grain boundaries have small misorientation angles suggests that percolative paths for strongly linked flow exist. Examination of maps of misorientation angles over small areas indicates that two-dimensional percolative paths among grains at the Ag/superconductor interface revealed by etching away the silver can indeed be found [25]. Moderate c-axis texture leaves many misaligned grains which insure that current flow is three-dimensional [15, 18] and increase the number of percolative connections.

With moderate c-axis alignment most grain boundaries do not involve pure rotations about a principal axis and have mixed character (i.e. have both tilt and twist components). The properties of such mixed grain boundaries have not been measured. While the microstructural origins of weak link behavior at grain boundaries are not fully known, there are two reasons to expect that small angle and CSL boundaries may be good. First, impurity and cation constituent segregation to grain boundaries is driven by grain boundary energy. Therefore, low energy boundaries should be cleaner and more stoichiometric, factors which have been shown to have a secondary effect on weak link behavior in $YBa_2Cu_3O_7$ [29, 30]. Of greater general importance are the changes in grain boundary structure with misorientation angle. Strain at small angle (typically less than 15°) and CSL boundaries is accommodated by a series of dislocations, the spacing between which is inversely related to the misorientation angle. The resulting strain field

at the grain boundary has periodically spaced regions of low strain through which it has been speculated [31] strongly linked current may flow. As the misorientation angle or deviation from ideal CSL increases the dislocation core spacing decreases and the areas of low strain decrease. For misorientation angles greater than about 15° dislocation cores overlap.

3.2. $TlBa_2Ca_2Cu_3O_{8+x}$ Deposits

High J_C $TlBa_2Ca_2Cu_3O_{8+x}$ deposits on yttria-stabilized ZrO_2 substrates have been examined by x-ray microdiffraction, transmission electron microscopy, and electron back scatter diffraction [21-23]. The superconducting phase was formed by vapor phase thallination of a spray-pyrolyzed thallium-free precursor deposit by procedures which have been described previously [3, 4]. Typically, the FWHM of a c-axis rocking curve is 1-2°, indicating very good c-axis texture, thickness is approximately 3 μm and grains tend to be 0.2 μm to 1 μm thick (in the c-direction) and 3 μm to 10 μm in the plane. J_C measured resistively with voltage contact spacing in the range of 1 to 4 mm (therefore spanning hundreds of grains) is typically 0.5 - 1 x 10^5 A/cm^2 in self-field at 77 K and has good field dependence [3, 4]. At 40 K in fields up to 9T J_C remains well above 10^4 A/cm^2 [1]. X-ray phi scans were used to study the local and macroscopic in-plane texture. A large x-ray beam (4 x 8 mm) which illuminated most of the specimen surface indicated random a-axis orientations, i.e., no macroscopic in-plane texture. However, restricted beams of 0.5 x 1 mm and 100 x 100μm showed a very high degree of in-plane texture. These results were interpreted as indicating the presence of colonies of grains with similar a-axis orientations. We note that these colonies are different from those in BSCCO, which consists of stacks of c-axis aligned grains which are connected by twist boundaries.

The colony microstructure was confirmed by EBSP determinations of the orientations of individual grains [23]. Figure 6 is an SEM image of the surface of a Tl-1223 deposit

showing growth ledges, pores, and second phase particles. Both polished and unpolished surfaces were successfully analyzed by EBSP. In neither case could grain boundaries be revealed in SEM, requiring the following procedure for mapping a-axis orientations. While observing the diffraction pattern the electron beam was moved in a line over the sample surface. When a shift in the pattern was observed the new pattern was recorded and analyzed to obtain the local crystalline orientation. Since the c-axes were very well aligned, the orientation of a grain can be represented by a single arrow in the a-direction. In Fig. 7, the a-axis directions are plotted for a 40 x 120 μm area. The beam was moved along parallel lines separated by 12 μm to obtain data over the rectangular grid. An arrow is plotted only where a shift in diffraction pattern was seen, i.e., after crossing a grain boundary. The spacing between arrows is roughly indicative of grain size, although surface irregularities prevented obtaining patterns in some areas, and therefore some shifts in orientation were missed. Clearly this area is within a single colony. The total spread in a-axis orientation is ~15-20°. Figure 8 shows a similar map over a somewhat larger area of the same sample. In this case an irregularly shaped colony intersection can be discerned clearly. The average a-axis orientations of the two colonies differ by ~35-40°. Figure 9 shows an EBSP map of another colony intersection. In this case there appears to be a gradual change of orientation across the intersection, and hence the colony boundary is not easily discerned. Larger, more complex regions contain a mixture of the three cases illustrated in Figs. 7-9. Colony dimensions in the plane appear to be in the range of 0.1 mm to 1 mm. Colonies have irregular shapes and therefore large areas of intersection. In these Tl-1223 deposits colony intersections are made up of a large number of c-axis tilt grain boundaries. Within a colony most grain boundaries have small misorientation angles and thus should not be weak links. We have proposed [21-23] that long range current transfer occurs through a percolative network of small angle grain boundaries at colony intersections. The number of such small angle grain boundaries should increase with the spread in orientation of grains within a colony and with any tendency for adjacent

colonies to have similar orientations as might result from a local bias of colony orientation. The FWHM of peaks in XRD azimuthal scans tends to be ~10-20°, indicative of a similar spread in a-axis orientation. Since Tl-1223 is tetragonal the maximum misorientation angle between c-axis aligned grains is 45°. Thus, if colonies are randomly oriented and each colony intersects several other colonies, it is probable that a significant fraction of intersection area will have overlapping grain orientation distributions. The critical current of a randomly generated lattice of colonies having a spread in a-axis orientation derived from x-ray diffraction measurements was simulated [32] using the limiting path method [33]. The model predicts significantly higher in-field J_C for a colony microstructure than for a c-axis textured deposit with random a-axis orientations.

The nature of grain boundaries at colony intersections appears to largely determine long-range J_C. It is thus important whether grain boundary misorientations at colony intersections are statistically determined by the grain orientation distributions in the adjacent colonies as assumed above or whether the distribution is biased by grain boundary energy or presently undefined aspects of the growth process. In Figs. 7-9 statistic are given for the fraction of small angle and CSL boundaries obtained by calculating angle/axis pairs for adjacent points along a horizontal line. As expected, in all areas a high fraction of boundaries are small angle. In Fig. 8, which includes a well defined colony intersection a high fraction of large angle boundaries are within the Brandon criterion [34] for an ideal CSL. Since most of these large angle boundaries are at the colony intersection, this result suggests that grain boundary energy may affect significantly grain boundary misorientations at colony intersections. Among the several specimens and areas examined the misorientation angle distributions vary considerably, but in all of these areas the population of CSL boundaries appears to be elevated.

4. DISCUSSION

The results presented demonstrate for both the Bi-2223 conductor and Tl-1223 deposits that small angle grain boundaries are present in much higher numbers than expected statistically from macroscopic textures. This result, in conjunction with the growing body of evidence that large angle boundaries (possibly excluding CSL boundaries) in most, if not all, oxide superconductors are weak-links, strongly suggests that long-range conduction occurs by percolation through a connected network of small angle (and perhaps CSL) boundaries. Critical current density is determined by local grain boundary misorientations, not macroscopic texture. Texture determines the probability that adjacent grains will have similar orientations. Grain boundary energy provides a driving force which skews the misorientation distribution toward small angle and probably CSL boundaries. The percolative paths in the two materials are very different. In the Tl-1223 deposits a very high density of small angle grain boundaries is associated with the colony microstructure, and long-range conduction depends on percolation through a much smaller population of small angle (and possibly CSL) boundaries at colony intersections. In Bi-2223 conductor a randomly distributed but smaller population of small angle boundaries is sufficient to ensure percolation of current. We have observed that J_C in Bi-2223 conductors does not correlate perfectly with the degree of c-axis alignment and second phase content as determined from x-ray diffraction and microscopic examination of polished cross-sections. We suggest that the population of small-angle boundaries is the "hidden variable" with which J_C correlates.

Percolation through a network of low energy boundaries is offered as a general model for long-range conduction in polycrystalline superconductors. This model lacks the specific drawbacks of previous models: conduction in the c-direction is not required, and grain boundary behavior is assumed to be the same in all high-T_C materials. In addition to the materials discussed here, the model also appears to explain strongly-

linked current flow in multifilamentary $YBa_2Cu_4O_8$ conductors prepared by the oxidation-of-metallic precursor method [5]. In that material x-ray diffraction indicates modest biaxial texture while selected area diffraction in TEM indicates a sharper local texture in the regions examined. This material appears to have yet another arrangement of grains leading to a connected network of small angle boundaries, the complete definition of which requires further study.

The proposed model for long-range conduction is based on the assumption that for clean grain boundaries $J_c(gb)$ is determined by the misorientation angle. It is recognized however that because structure and superconducting properties are anisotropic, the axis of rotation and grain boundary plane may affect $J_c(gb)$. These results indicate the importance of further studies of the effects of grain boundary geometry on $J_c(gb)$.

5. ACKNOWLEDGMENTS

This research is sponsored by the U.S. Department of Energy Office of Advanced Utility Concepts-Superconducting Technology Program under contract DE-AC05-84OR21400 with Martin Marietta Energy Systems, Inc. The authors thank D. K. Christen for helpful discussions and D. Dingley and T. Mason for help in acquiring and analyzing electron back scatter diffraction patterns.

REFERENCES

1. K. Sato et al., IEEE Transactions on Magnetics **27**, 1231 (1991).

2. J. Tenbrink, K. Heine, and H. Krauth, Cryogenics **30**, 422 (1990).

3. J. E. Tkaczyk, J. A. DeLuca, P. L. Karas, P. J. Bednarczyk, M. F. Garbauskas, R. H. Arendt, K. W. Lay, and J. S. Moodera, Appl. Phys. Lett. 61, **610** (1992).

4. J. A. DeLuca, P. L. Karas J. E. Tkaczyk, P. J. Bednarczyk, M. F. Garbauskas, C. L. Briant, and D. B. Sorensen, Physica C **205**, 21 (1993).

5. L. J. Masur, E. R. Podtburg, C. A. Craven, A. Otto, Z. L. Wang, D. M. Kroeger, J. Y. Coulter and M. P. Maley. To be published in Physica C.

6. D. Dimos, P. Chaudhari, J. Mannhart, and F. K. LeGoues, Phys. Rev. Lett. **61**, 219 (1988); D. Dimos, P. Chaudhari, and J. Mannhart, Phys. Rev. B **41**, 4038 (1990).

7. R. Gross and B. Mayer, Physica C **180**, 235 (1991).

8. J. Mannhart and C. C. Tsuei, Z. Phys. B **77**, 53 (1989).

9. A. P. Malozemoff, in High Transition Temperature Compounds II, edited by S. H. Whang, A. DasGupta, and R. B. Laibowitz (TMS, Warrendale, PA, 1990), p. 3.

10. J. W. Ekin, T. M. Larson, A. M. Hermann, Z. Z. Sheng, K. Togano, H. Kumakura, Physica C **160**, 489 (1989)

11. J. W. Ekin, H. R. Hart, Jr., and A. R. Gaddipati, J. Appl. Phys. **68**, 2285 (1990).

12. L. N. Bulaevskii, J. R. Clem, L. I. Glazman, and A. P. Malozemoff, Phys. Rev. B **45**, 2445 (1992).

13. L. L. Daemen, L. N. Bulaevskii, M. P. Maley, and J. Y. Coulter, Phys. Rev. B 47, 11291 (1993).

14. A. Umezawa, Y. Feng, H. S. Edelman, Y. E. High, D. C. Larbalestier, Y. S. Sung and E. E. Hellstrom, Physica C 198, **261** (1992).

15. B. Hensel, J. C. Grivel, A. Jeremie, A. Perin, and A. Pollini, and R. Flukiger, Physica C. **205**, 329 (1993).

16. S. Jin, R. B. VanDover, T. M. Tiefel, J. E. Graebner, and N. D. Spencer, Appl. Phys. Lett. **58**, 868 (1991); S. Jin, T. H. Tiefel, R. B. VanDover, J. E. Graebner, T. Siegrist, and G. W. Kammlott, Appl. Phys. Lett. To be published.

17. A. D. Caplin, S. M. Cassidy, L. F. Cohen, M. N. Cuthbert, J. R. Laverty, G. K. Perkins, S. X. Dou, Y. C. Guo, and H. K. Liu, pg. 279, Proc. of the 1993 TMS Fall Meeting, Oct. 17-21, Pittsburgh, PA, edited by U. Balachandaran, E. W. Collings and A. Goyal.

18. J. H. Cho, M. P. Maley, J. O. Willis, J. Y. Coulter, L. N. Bulaevskii, P. Haldar, and L. R. Motowidlo, Appl. Phys. Lett. **64**, 3030 (1994).

19. T. Nabatame, S. Koike, O. B. Hyun, I. Hirabayashi, H. Suhara and K. Nakamura, Appl. Phys. Lett. **65**, 776 (1994).

20. A. Goyal. et al., Manuscript in preparation.

21. D. M. Kroeger, A. Goyal, E. D. Specht, Z. L. Wang, J. E. Tkaczyk, J. A. Sutliff, and J. A. DeLuca, Appl. Phys. Lett. **64**, 1 (1994).

22. E. D. Specht, A. Goyal, D. M. Kroeger, J. A. DeLuca, J. E. Tkaczyk, C. L. Briant and J. A. Sutliff, Physica C **226**, 76 (1994).

23. A. Goyal, E. D. Specht, Z. L. Wang, D. M. Kroeger, J. A. Sutliff, J. E. Tkaczyk, J. A. DeLuca, L. Masur, and G. N. Riley, Jr. To be published in J. of Electronic Materials, 1994.

24. J. K. MacKenzie, Biometrika **45**, 229 (1958).

25. A. Goyal et al., Manuscript in preparation, 1994.

26. A. Sequeira, J. V. Yakhmi, R. M. Iyer, H. Rajagopal and P. Sastry, Physica C **167**, 291 (1990).

27. R. M. Hazen in "Physical Properties of High Temperature Superconductors, Vol. II," edited by D. M. Ginsberg, World Scientific, Teaneck, NJ (1990).

28. J. L. Wang, X. Y. Lin, R. J. Kelley, S. E. Babcock, D. C. Larbalestier, and M. D. Vaudin, Physica C **230**, 189 (1994).

29. D. M. Kroeger, A. Choudhury, J. Brynestad, R. K. Williams, R. A. Padgett, and W. A. Coghlan, J. Appl. Phys. **64**(1), 331 (1988).

30. K. B. Alexander, D. M. Kroeger, J. Bentley and J. Brynestad, Physica C **180**, 337 (1991).

31. S. E. Babcock and D. C. Larbalestier, J. Mater. Res. **5**, 919 (1990).

32. E. D. Specht, A. Goyal, D. M. Kroeger, J. A. DeLuca, J. E. Tkaczyk, C. L. Briant, and J. A. Sutliff. Submitted to Appl. Phys. Lett.

33. J. Rhyner and G. Blatter, Phys. Rev. B **40**, 829 (1989).

34. D. G. Brandon, Acta Metall. **14**, 1479 (1956).

FIGURE CAPTIONS

Fig. 1. Distribution of misorientation angles for the 20,000 "grain boundaries" which could be formed among 200 randomly oriented grains. The shape of the histogram agrees well with the calculated curve of Mackenzie [23].

Fig. 2. Fraction of misorientation angles less than a given angle, obtained from 20,000 simulated grain boundaries for cubic, tetragonal and orthorhombic symmetries.

Fig. 3. The effect of macroscopic c-axis texture on the misorientation angle distribution from simulations for tetragonal symmetry. In randomly selecting the 200 grain set from which grain boundaries were formed, deviations of the c-axes from perpendicular to the sample plane were restricted as indicated.

Fig. 4. SEM image of the Bi-2223 surface of a filament revealed by etching away the silver from a multifilamentary powder-in-tube specimen. Grain boundaries are clearly visible, permitting determinations by EBSP of the orientations of contiguous grains.

Fig. 5. Statistics for small angle and coincident site lattice boundaries for a Bi(Pb)-2223 conductor.

Fig. 6. SEM image of the free surface of a polycrystalline $TlBa_2Ca_2Cu_3O_{8+x}$ deposit. Grain boundaries cannot be discerned.

Fig. 7. Arrow map of the projections of a-axes on to the sample plane over a 40 x 120 μm area on a Tl-1223 deposit. The arrows have similar directions, indicating the area is within a colony. The e-beam was scanned along a horizontal line. When the pattern changed, indicating a grain boundary was traversed, the new grain orientation was calculated and the a-axis projection plotted. The angle/axis pairs were also calculated. For 80% of the boundaries $\Theta < 10°$.

Fig. 8 a-axis arrow map for an area which contains a sharp colony intersection, indicated by the hand-drawn curve. For 75% of boundaries $\Theta < 10°$, and 54% of boundaries with $\Theta < 15°$ are within the Brandon criterion for an ideal CSL.

Fig. 9 a-axis arrow map for an area in which orientation appears to change gradually without a well-defined colony boundary. 52% of boundaries have $\Theta < 10°$, and 14% of large angle boundaries are within the Brandon criterion for an ideal CSL.

Fig. 1

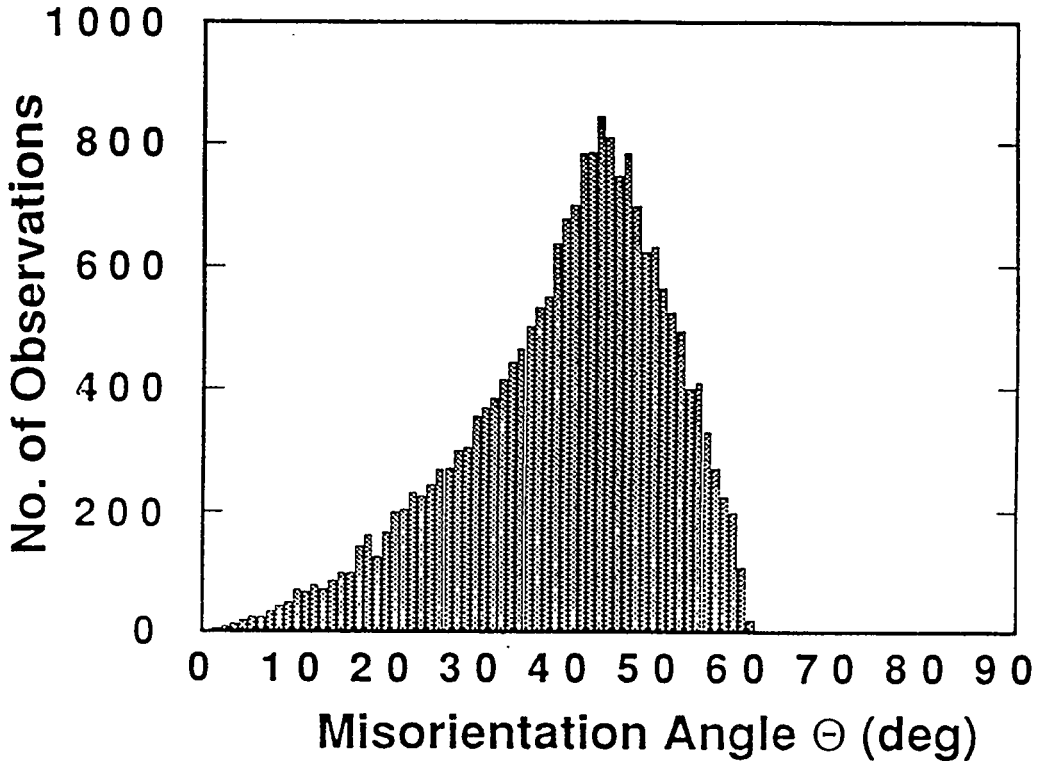
No. of Observations
1000
800
600
400
200
0
0 10 20 30 40 50 60 70 80 90
Misorientation Angle Θ (deg)

g. 2

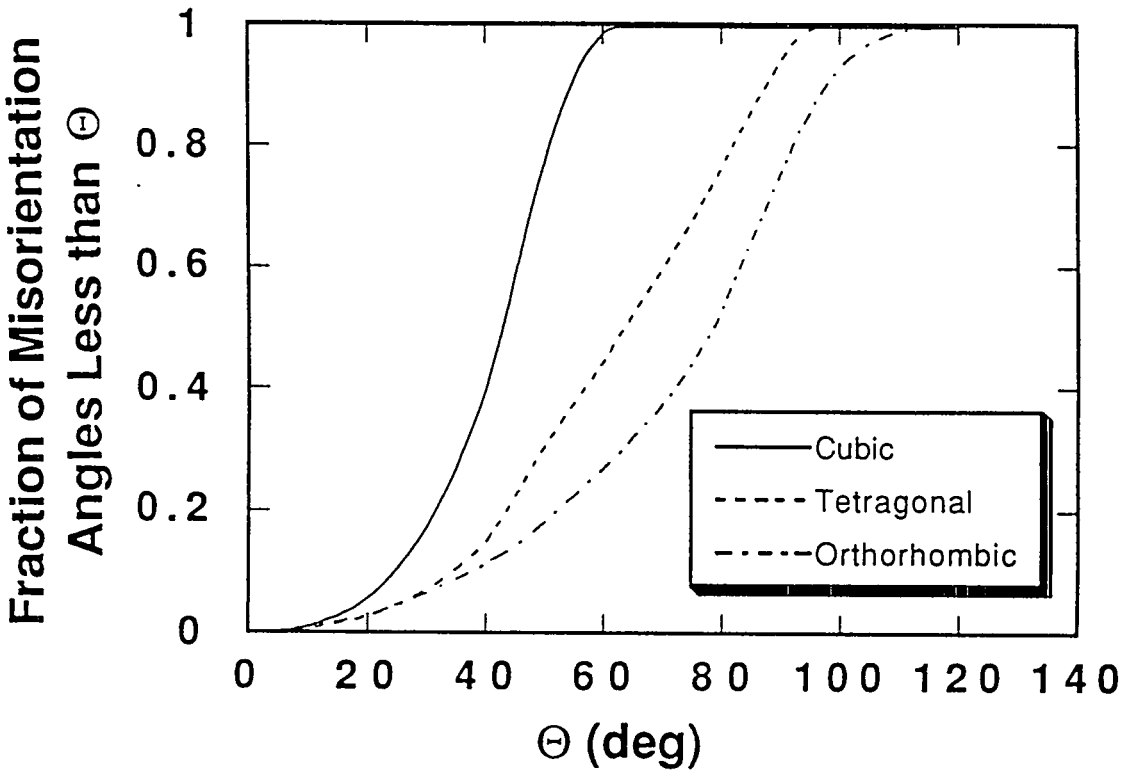
Fraction of Misorientation Angles Less than Θ
1
0.8
0.6
0.4
0.2
0
0 20 40 60 80 100 120 140
Θ (deg)
Cubic
Tetragonal
Orthorhombic

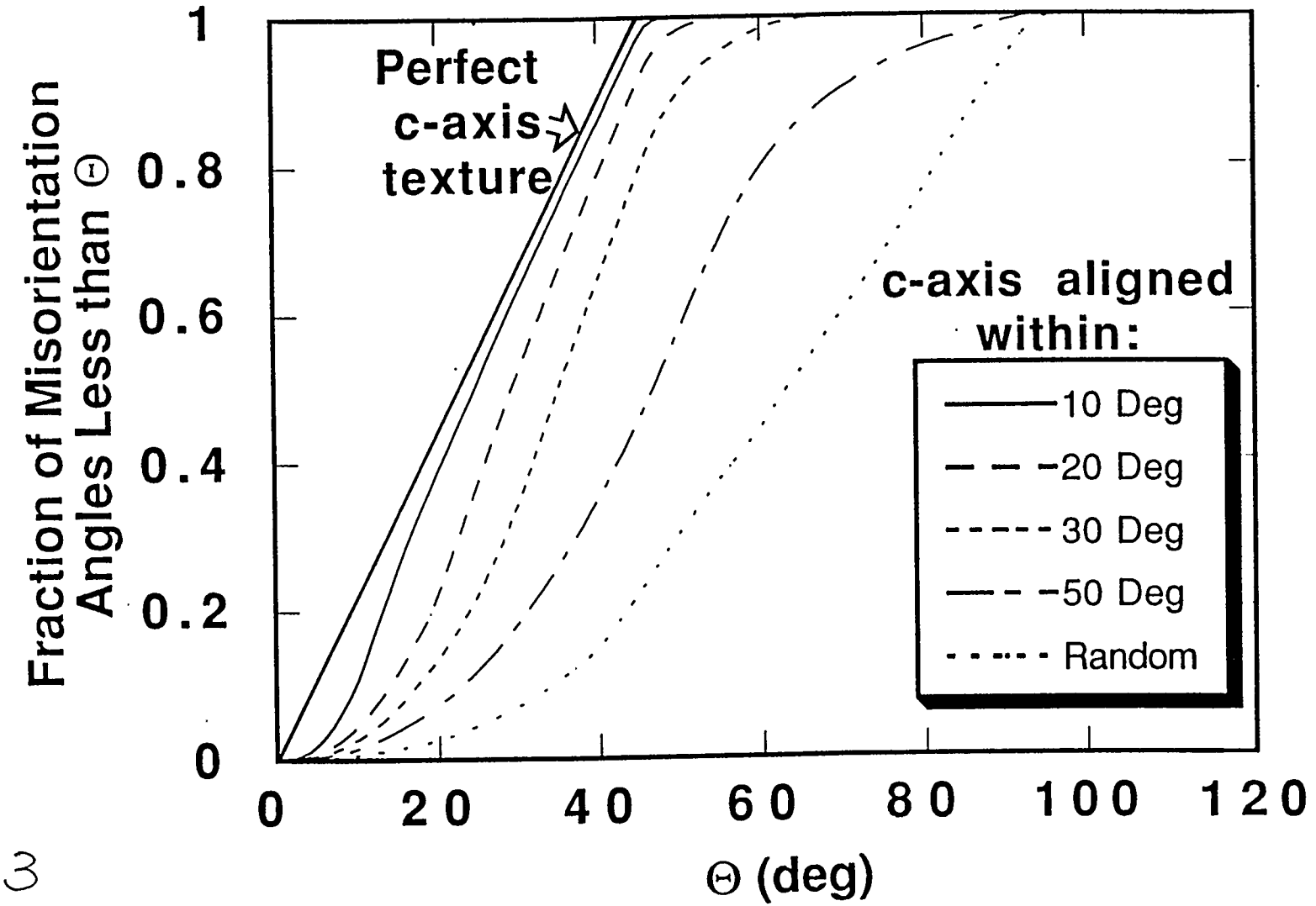
Fraction of Misorientation Angles Less than Θ
1
0.8
0.6
0.4
0.2
0
Perfect c-axis texture
c-axis aligned within:
10 Deg
20 Deg
30 Deg
50 Deg
Random
0
20
40
60
80
100
120
Θ (deg)

Fig. 3

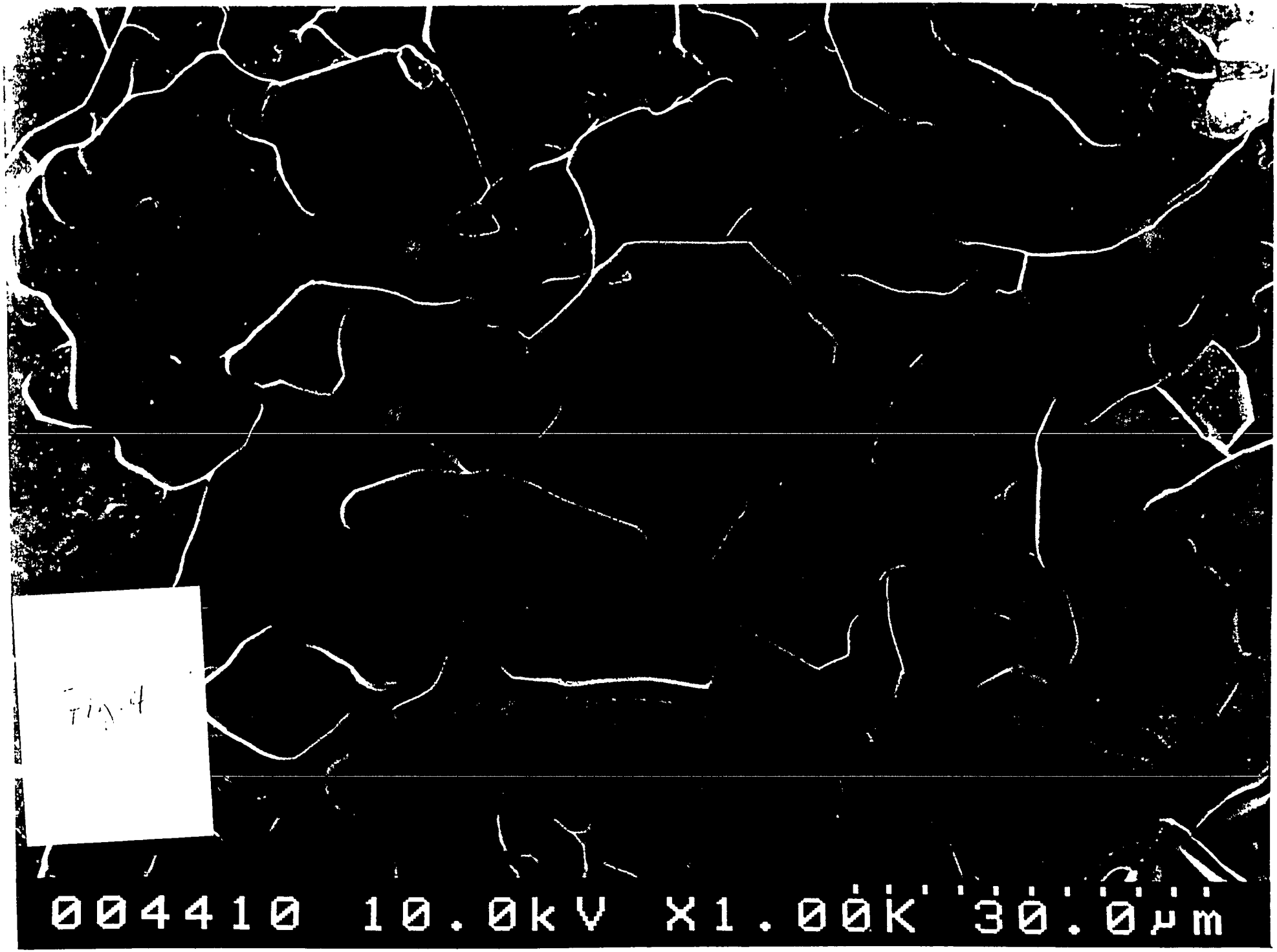
004410 10.0kV X1.00K 30.0µm

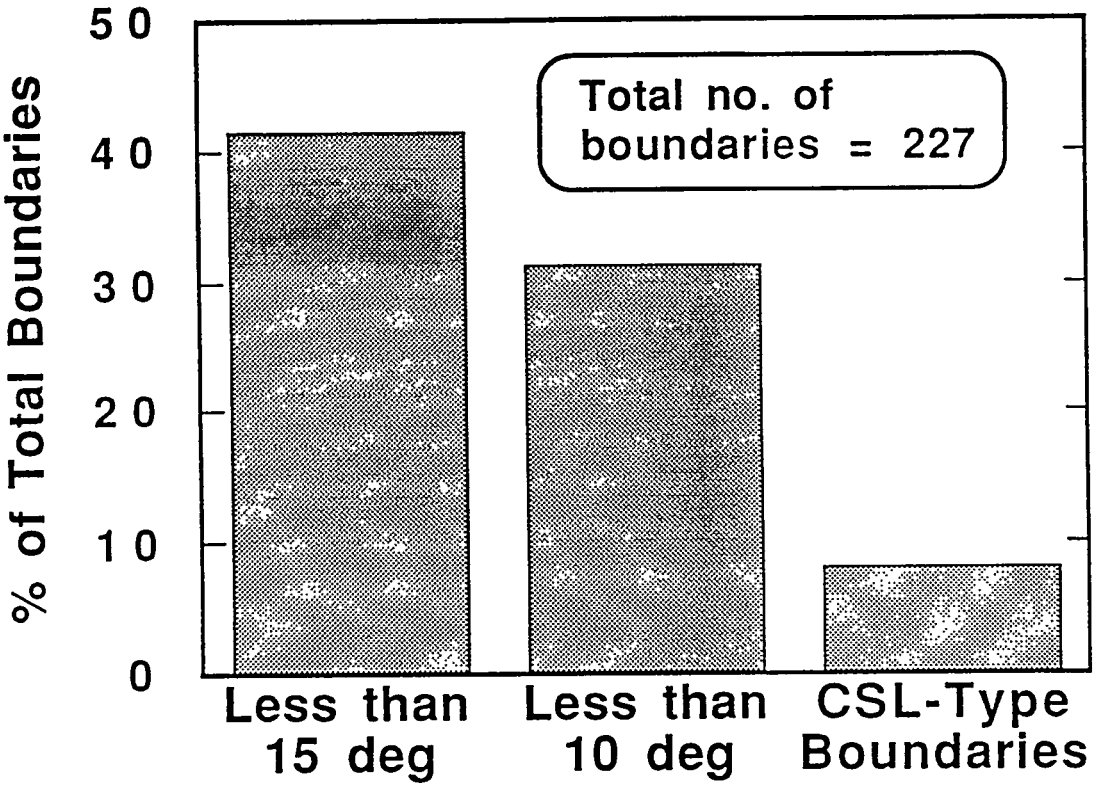
% of Total Boundaries
50
40
30
20
10
0
Total no. of boundaries = 227
Less than 15 deg
Less than 10 deg
CSL-Type Boundaries

Fig. 5

Fig. 6

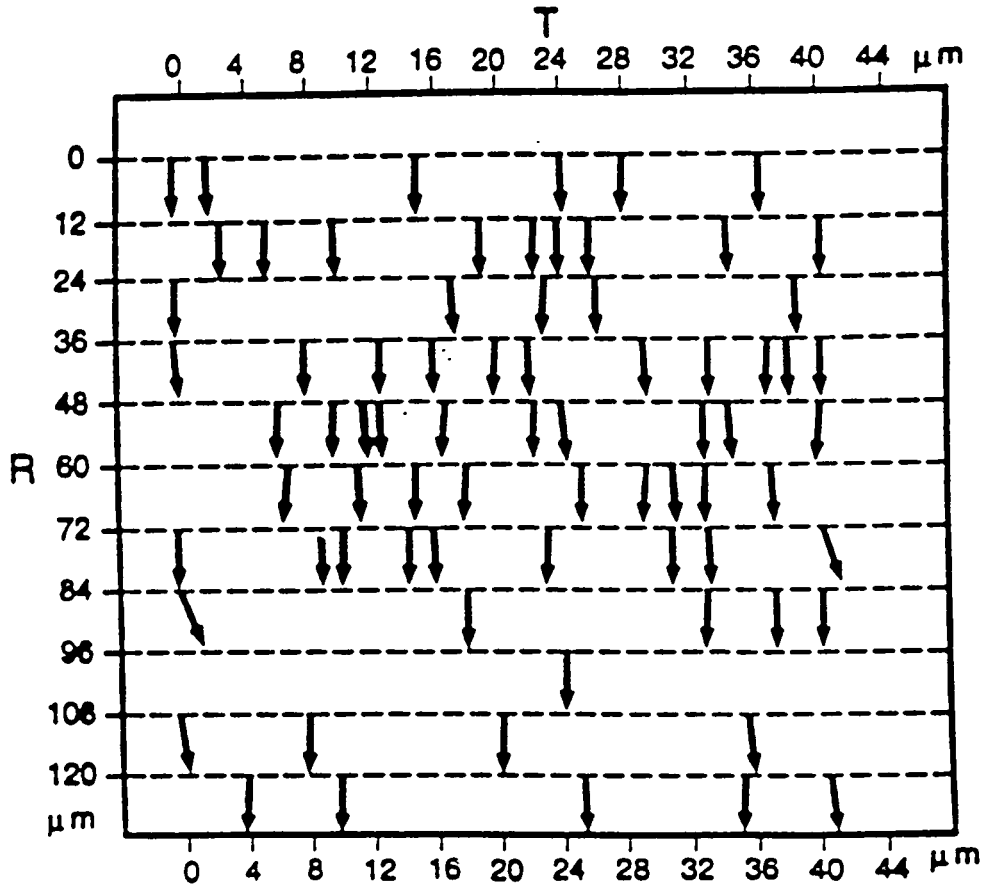
T
0 4 8 12 16 20 24 28 32 36 40 44 µm
R
0
12
24
36
48
60
72
84
96
108
120
µm
0 4 8 12 16 20 24 28 32 36 40 44 µm

Fig. 7

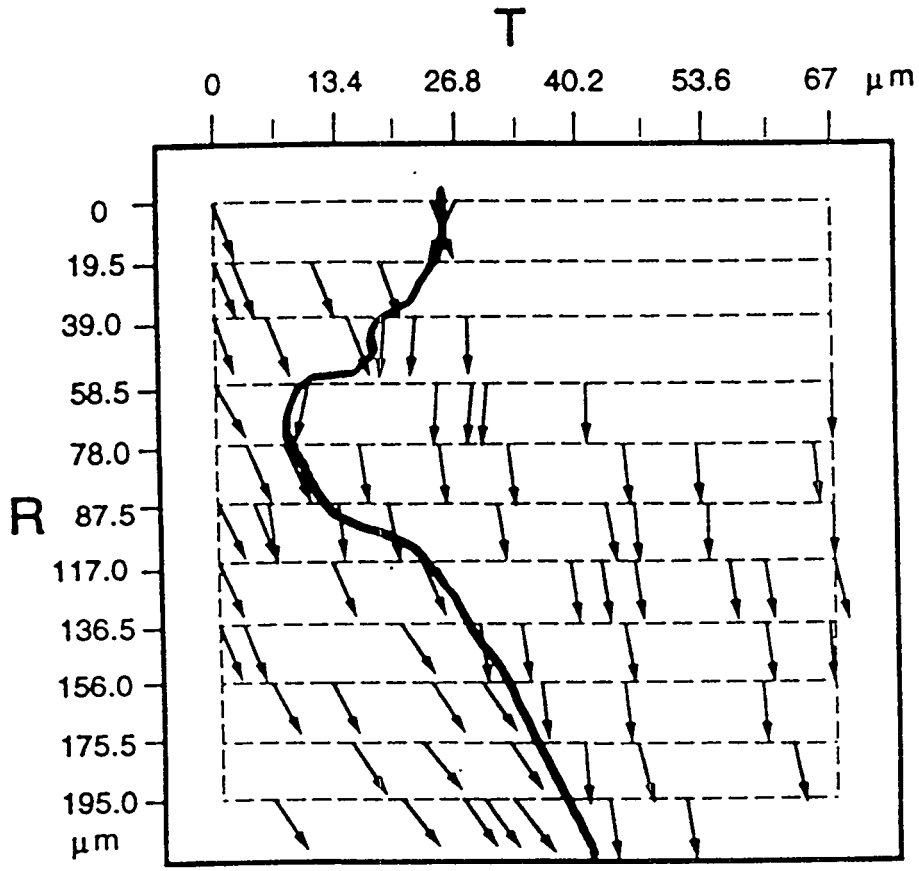
T
0
13.4
26.8
40.2
53.6
67 µm
R
0
19.5
39.0
58.5
78.0
87.5
117.0
136.5
156.0
175.5
195.0
µm

Fig. 8

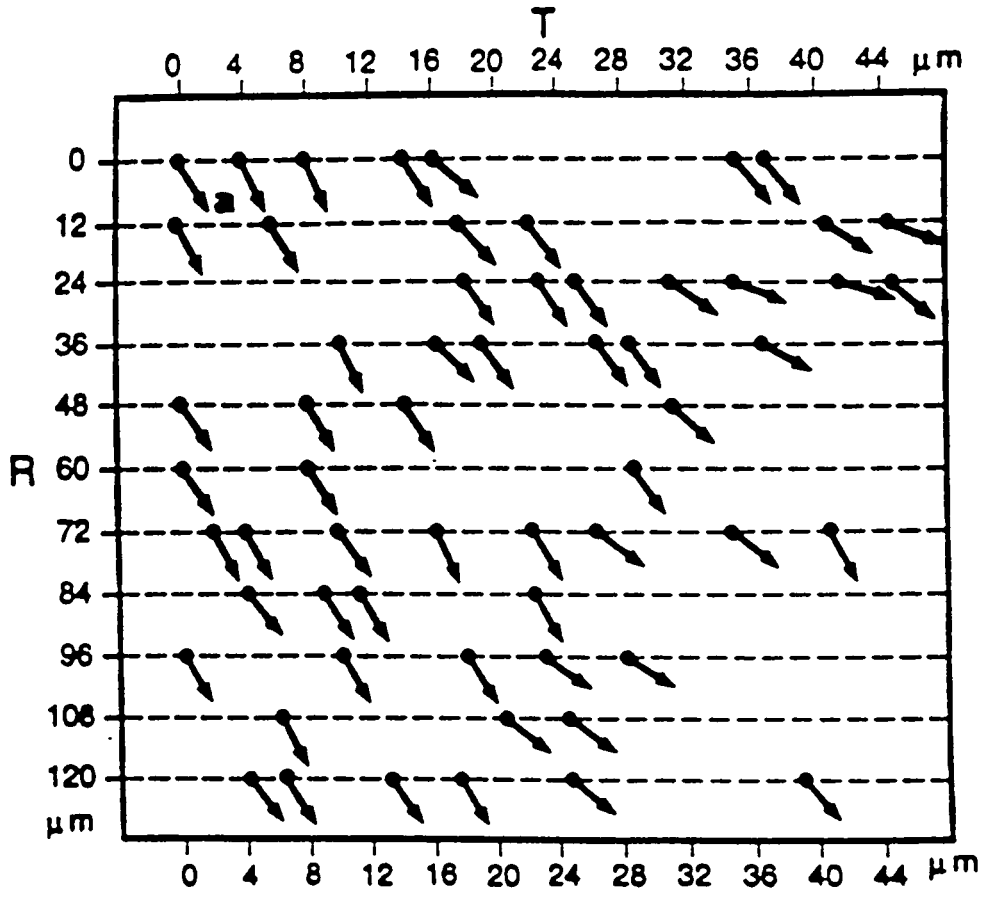
T
0 4 8 12 16 20 24 28 32 36 40 44 µm
a
R
0
12
24
36
48
60
72
84
96
108
120
µm
0 4 8 12 16 20 24 28 32 36 40 44 µm

Fig. 9